Published in final edited form as:
Biochemistry. 2013 September 24; 52(38): 6595–6600. doi:10.1021/bi400952m.

A Large Solvent Isotope Effect on Protein Association Thermodynamics

Christopher Eginton and **Dorothy Beckett***
Department of Chemistry & Biochemistry, College of Computer, Mathematical & Natural Sciences, University of Maryland, College Park, MD 20742

Abstract

Solvent reorganization can contribute significantly to the energetics of protein:protein interactions. However, our knowledge of the magnitude of the energetic contribution is limited, in part, by a dearth of quantitative experimental measurements. The biotin repressor forms a homodimer as a prerequisite to DNA binding to repress transcription initiation. At 20°C the dimerization reaction, which is thermodynamically coupled to binding of a small ligand, bio-5'-AMP, is characterized by a Gibbs free energy of -7 kcal/mole. This modest net dimerization free energy reflects underlying very large opposing enthalpic and entropic driving forces of +41±3 and -48±3 kcal/mole. The thermodynamics have been interpreted as indicating coupling of solvent release to dimerization. In this work this interpretation has been investigated by measuring the effect of replacing H_2O with D_2O on the dimerization thermodynamics. Sedimentation equilibrium measurements performed at 20°C reveal a solvent isotope effect of -1.5 kcal/mole on the Gibbs free energy of dimerization. Analysis of the temperature dependence of the reaction in D_2O indicates enthalpic and entropic contributions of +28 and -37 kcal/mole, respectively, considerably smaller than the values measured in H_2O. These large solvent isotope perturbations to the thermodynamics are consistent with a significant contribution of solvent release to the dimerization reaction.

Protein:protein interactions are central to a broad range of biological processes including signal transduction[1], transcription regulation[2] and morphogenesis.[3] Although the intrinsic chemistry of the interacting protein partners is important in determining the strength of an interaction, water, either through its release into the bulk upon interface formation or its direct participation in the interface, is also integral to protein:protein interactions. Moreover, simulations predict that the interplay of protein sequence with solvent profoundly influences protein assembly reactions[4]. Despite the widespread appreciation of its significance, experimental determination and computational prediction of the energetic contribution of solvent reorganization remains a challenge for both understanding the physical chemistry of protein:protein interactions and for design of novel interactions[5].

The *E. coli* protein BirA forms a homodimer prior to binding to DNA to regulate transcription initiation[6]. The dimerization reaction is thermodynamically coupled to small molecule bio-5'-AMP binding, which renders the protein:protein interaction more favorable by -4 kcal/mole (Fig. 1).[7; 8] The equilibrium dimerization constant for bio-5'-AMP bound BirA, holoBirA, is 6 μM at 20°C, 200 mM KCl, pH 7.5, which corresponds to a modest Gibbs free energy of -7 kcal/mole[8]. By contrast, van't Hoff analysis of the temperature-dependence of the reaction indicates very large opposing enthalpic, $\Delta H°_{DIM}$, and entropic, $-T\Delta S°_{DIM}$, driving forces of +41 and -48 kcal/mole, respectively, at 20°C[9]. Furthermore, the

*Corresponding author: phone: 301-405-1812, dbeckett@umd.edu.

linearity of the Van't Hoff plot obtained from analysis of the temperature-dependence of the dimerization reaction is consistent with the absence of a heat capacity change in the reaction.

The large opposing enthalpies and entropies of holoBirA dimerization are consistent with solvent release upon dimer formation.[9; 10] The enthalpic penalty may reflect the cost of water removal from the dimerization surface concomitant with formation of the interface[11]. Likewise, the favorable entropy is consistent with release of bound water to the bulk upon dimerization. The chemistry of the dimerization surface, which contains a number of polar and charged groups, is consistent with a large enthalpic penalty of removing surface-bound water in the course of dimerization[12]. Analysis of the dimer interface, in which 40% of the buried groups are polar, indicates the presence of 16 hydrogen bonds and 4 salt bridges.[13; 14] Furthermore, few water molecules are located in the interface. However, given the net unfavorable dimerization enthalpy is 41 kcal/mole, this structural interpretation of the thermodynamics assumes a desolvation penalty that is much larger than the favorable enthalpy associated with formation of combined inter-solvent hydrogen and protein:protein interface bonds.

A number of experimental approaches have been used to investigate the contribution of water reorganization to biomolecular interactions. Addition of osmolytes allows measurements of the dependence of the reaction on water activity, thus providing information about the number of waters released or taken up in the course of binding. However, a potential complication to interpretation of the results lies in the preferential interaction of the osmolyte with one or more of the interacting partners[15]. The volume change obtained from measuring the response of the equilibrium constant for an interaction to changes in hydrostatic pressure can be interpreted in terms of the linkage of water binding/release to the equilibrium process[16]. Pressure perturbation calorimetry also provides a means of estimating the role of water reorganization in biomolecular interactions[17]. Finally, because of the distinct hydrogen bonding properties of the two, measurements of the solvent isotope effect of replacing H_2O with D_2O have been used to estimate the contribution of water reorganization to protein:protein association[18].

In this work the role of solvent reorganization in holoBirA dimerization has been probed by measuring the consequences for the reaction of replacing H_2O with D_2O. Sedimentation equilibrium measurements performed on wild type and single amino acid variants of BirA reveal that dimerization is consistently more favorable by approximately -1.5 kcal/mole in D_2O than in H_2O. Van't Hoff analysis of the temperature-dependence of the dimerization equilibrium measured in heavy water indicates linear behavior that yields an unfavorable dimerization enthalpy of 28 kcal/mole, 13 kcal/mole less than that measured in H_2O. This enthalpy decrease is accompanied by similarly large decrease in the favorable dimerization entropy. The results are consistent with a contribution of solvent reorganization to the holoBirA dimerization energetics.

Materials and Methods

Chemicals and Biochemicals

All chemicals used in buffer preparation were at least reagent grade. The bio-5'-AMP was synthesized and purified as previously described.[19; 20] The standard buffer (10mM Tris HCl, 200mM KCl, and 2.5mM $MgCl_2$) prepared in D_2O was adjusted to a pD of 7.5 using a meter reading of 7.1 to correct for the effect of deuterium on glass electrodes.[21]

Protein Preparation

BirA protein variants were prepared and purified as previously described[22; 23] and the purity of each was estimated to be >95% based on coomassie brilliant blue staining of samples

subjected to SDS-polyacrylamide gel electrophoresis. Protein concentrations were determined spectrophotometrically at 280 nm using a molar extinction coefficient of 47,510 M^{-1} cm^{-1} calculated from the amino acid composition.[24] The fractional activity of each protein is >90% as determined by stoichiometric binding titrations with bio-5'-AMP monitored by steady-state fluorescence spectroscopy.[20]

Sedimentation Equilibrium

The self-association of each BirA variant complexed with bio-5'-AMP was measured by equilibrium analytical ultracentrifugation using a Beckman Coulter Optima XL-I Analytical Ultracentrifuge. Proteins were first exchanged into SB:D_2O using Micro Bio-Spin 6 chromatography columns (BioRad) as described by the manufacturer. For each measurement, protein prepared at three different concentrations was combined at stoichiometric conditions with bio-5'-AMP at a final molar ratio of 1:1.5. Equilibrium dissociation constants for binding of the ligand to the BirA variants range from picomolar to nanomolar [22;23]. For each variant and/or solvent condition the protein concentrations employed varied depending on the strength of the dimerization reaction. Lower concentrations were employed for tightly dimerizing systems and higher concentrations for weakly dimerizing systems with the goal of optimizing representation of the dimer and monomer species in the concentration versus radial distance profiles. Samples were centrifuged in cells equipped with 12 mm six-hole or 3 mm two-hole charcoal-filled Epon centerpieces with quartz windows in a four-hole An-60 rotor (Beckman Coulter). Prior to centrifugation, the filled sample cells and rotor were incubated at the specified temperature for 1 hour. Centrifugation was carried out at three rotor speeds ranging from 18,000 to 24,000 rpm. After reaching equilibrium, scans were acquired with a step size of 0.001 cm with 5 averages at either 295 or 300 nm. At these wavelengths the contribution from the absorbance of the adenosine moiety of bio-5'-AMP was avoided and, for samples prepared at very high protein concentrations, the total absorbance was in the linear range of the detection system.

Data Analysis

The absorbance *versus* radius profiles obtained for each scan were analyzed with WinNONLIN [25] using a single species model to obtain σ, the reduced molecular weight, from which the weight average molecular weight was calculated using the following equation:

$$\sigma = \frac{kM(1 - \frac{\bar{\nu}}{k}\rho)\omega^2}{RT} \quad (1)$$

where M is the molecular weight, k is the proportionality constant for the associated increase in molecular weight and decrease in the partial specific volume that occurs as a result of deuterium exchange into the protein[26], $\bar{\nu}$ is the protein partial specific volume, ρ is the buffer density, ω is the angular velocity of the rotor, R is the gas constant and T is the temperature in Kelvin. Based on a buffer composition of 95% (v/v) D_2O, a value for k of 1.0147 was used[27]. The partial specific volume of the BirA monomer is 0.755 mL/g[7] and the density was calculated from the buffer composition at the appropriate temperature using Sednterp (http://sednterp.unh.edu/). Absorbance *versus* radius profiles were also globally analyzed to obtain the equilibrium association constant for dimerization, K_a, using the following monomer-dimer model:

$$C_t(r)=\delta+C_{mon}(r_o)e^{\sigma_{mon}(\frac{r^2}{2}-\frac{r_o^2}{2})}+K_a(C_{mon}(r_o))^2e^{2\sigma_{mon}(\frac{r^2}{2}-\frac{r_o^2}{2})} \quad (2)$$

in which C_t is the total concentration at each radial position r, δ is the baseline offset, which was allowed to float in the analysis, and $C_{mon}(r_o)$ is the monomer concentration at reference radial position, r_o. For measurements performed at 20°C, the σ_{mon} value used in calculations performed for wild type and variant proteins is the measured value in D_2O buffer for wild type apoBirA. In analysis of data acquired at other temperatures, the σ_{mon} value was adjusted for accompanying changes in the solvent density. In all analyses the reduced molecular weight of the dimer was assumed to be twice that of the monomer. The quality of each fit was assessed from the magnitude of the square root of the variance and the distribution of the residuals of the fit about zero.

Results

HoloBirA dimerization reaction is more favorable in D_2O than in H_2O

The equilibrium dimerization constant of wild type holoBirA at 20°C in standard buffer (10mM Tris HCl, 200mM KCl, and 2.5mM $MgCl_2$) prepared with D_2O (SB:D_2O) was measured using sedimentation equilibrium. Initial analysis of the concentration versus radial position curves acquired at three loading concentrations and three speeds indicated weight average molecular weights higher than that expected for the monomer (Figure 2). Global analysis using a monomer-dimer model yielded a best-fit equilibrium dissociation constant for dimerization of 5 ±5 x10^{-7} M, indicating 12-fold tighter dimerization in SB:D_2O than in SB:H_2O (Table 1).

The magnitude of the D_2O effect on holoBirA self-association is conserved

The generality of the D_2O effect on holoBirA self-association energetics was investigated by performing measurements on the single alanine substituted variants, T195A and V219A. These particular variants were chosen based on the distinct locations of the substituted residues in the dimer structure and their altered dimerization energetics in H_2O relative to wild type BirA. The T195 residue is located at the core of the dimer interface and V219 is on the dimer surface in a loop that folds over the adenylate moiety of bio-5'-AMP (Figure 3A). The equilibrium dissociation constants for dimerization of the T195A and V219A variants in SB:H_2O buffer at 20°C are 80 and 100 μM, respectively[22; 23].

Sedimentation measurements for the bio-5'-AMP-bound forms of T195A and V219A in SB:D_2O were performed as described for wild type BirA. The high affinities of both proteins for the ligand ensure that they are quantitatively in the holo-form at the concentrations employed for the measurements. Global nonlinear least squares analysis of the data yielded equilibrium dissociation constant for dimerization in D_2O buffer that are 10-fold smaller than those measured in H_2O buffer. Thus, similar to the effect observed for wild type holoBirA dimerization, the Gibbs free energies calculated form the resolved equilibrium constants indicate -1.4 to -1.5 kcal/mole enhancements in dimerization of the variants resulting from transfer of the reaction from SB:H_2O to SB:D_2O (Fig. 3B).

The magnitude of the coupling of ligand, bio-5'-AMP, binding to BirA dimerization is preserved in D_2O

BirA dimerization is thermodynamically coupled to bio-5'-AMP binding with a difference in the dimerization free energy for the liganded, holoBirA, and unliganded, apoBirA, in SB:H_2O of -4 kcal/mole[8]. The coupling in D_2O was investigated by performing sedimentation measurements on apoBirA prepared in SB:D_2O. In contrast to the holoBirA

samples, which were prepared at low micromolar concentrations, the weak apoBirA dimerization necessitated measurements on samples prepared in the 100 micromolar concentration range. Global analysis of the data using a monomer-dimer model yielded an equilibrium dissociation constant of 600 μM, corresponding to a Gibbs free energy of -4.3 kcal/mole, -1.5kcal more favorable than the value estimated for apoBirA in SB:H_2O.[8; 9] Calculation of the coupling free energy or $\Delta G°_{C,DIM}$ from the dimerization free energies obtained for apo and holoBirA in SB:D_2O yields a value of −4.2±0.5, identical, within error, to that obtained in SB:H_2O.

Enthalpic and entropic driving forces for dimerization in D_2O differ significantly from those measured in H_2O

In SB:H_2O at 20°C the modest holoBirA dimerization free energy results from large opposing enthalpic (ΔH°) and entropic (-TΔS°) contributions of +41 and -48 kcal/mole, respectively[9]. The solvent isotope effect on this thermodynamic signature was investigated by performing sedimentation measurements in SB:D_2O at temperature ranging from 5 to 20°C. The tight dimerization at higher temperatures precluded measurements above 20°C. At each temperature the data were acquired at three rotor speeds on samples prepared at three concentrations. At all temperatures the data are well-described by the monomer-dimer model and, as observed in SB:H_2O, the dimerization becomes tighter with increasing temperature (Fig. 4).[9] The dimerization free energies calculated from the resolved equilibrium constants reveal that increasing the temperature from 5 to 20°C renders the reaction more favorable by -1 kcal/mole. Van't Hoff analysis of the data indicates a linear relationship (Fig. 4) that yields a temperature-independent enthalpy, $\Delta H°_{DIM}$, of 28 ± 3 kcal/mol. The entropic contributions to the dimerization free energy, calculated using the expression $\Delta G°_{DIM} = \Delta H° - T\Delta S°$, are large and favorable over the entire temperature range (Fig. 5). As observed in SB:H_2O, holoBirA dimerization in SB:D_2O is characterized by a large unfavorable enthalpy and large favorable entropy. However, the absolute values of the two energetic parameters in D_2O are markedly more modest than in H_2O.

Discussion

BirA dimerization is enhanced in D_2O relative to H_2O

HoloBirA self-association in D_2O is energetically more favorable than in H_2O. Sedimentation equilibrium measurements of wild type holoBirA dimerization indicate a 12-fold decrease in the equilibrium dissociation constant in D_2O relative to H_2O, corresponding to a -1.5 kcal/mole enhancement in the dimerization free energy. Measurements performed on two BirA variants with single alanine substitutions as well as apoBirA indicate enhancements of identical magnitude. The distinct locations of the two substitutions in the 3-dimensional structure of BirA structure underscore the general effect of D_2O on the reaction. The T195A substitution is located in a loop in the dimerization interface. By contrast, the V219A substitution is in a surface loop that folds over the adenylate moiety of the ligand bio-5'-AMP, 24 Å away from the interface.[12]

Although holoBirA dimerization in D_2O is enhanced relative to the reaction in H_2O no effect on the linkage between corepressor binding and dimerization is observed. Bio-5'-AMP, enhances BirA dimerization in both H_2O and D_2O with a coupling free energy in of -4.0±0.3 kcal/mol, a result is consistent with the general effect of the heavier solvent on dimerization. However, the coupling free energy in H_2O was determined in buffer containing 50 mM KCl rather than the 200 mM KCl used in the current studies[8]. Thus, the conclusion that coupling free energies are equivalent in the two solvents assumes no influence of salt concentration on the coupling. The measured modest effect of monovalent salt concentration on holoBirA dimerization supports this assumption[9].

Previous studies indicate increases in self-association in D_2O relative to H_2O for several proteins including phycocyanin[28], glutamate dehydrogenase[29], and α-chymotrypsin[30]. For the limited number of studies that provided quantitative information, the magnitude of the effect varies. For example, at 4°C self-association of tobacco mosaic virus coat protein is modestly enhanced by 3-fold in D_2O relative to H_2O.[31] A 10-fold enhancement of β-lactoglobulin A self-association is observed in heavy water, similar in magnitude to the effect on BirA dimerization [32].

The thermodynamics in H_2O and D_2O are consistent with coupling of solvent release to holoBirA dimerization

The measurements of holoBirA dimerization as a function of temperature in heavy water provide additional support for a significant contribution of solvent release to the energetics of the process. The dimerization enthalpies obtained in SB:H_2O and SB:D_2O are 41±3 and 28±3 kcal/mol, respectively. At 20°C the entropic contributions, -TΔS°, to dimerization free energy, are -48 and -36 kcal/mole, respectively, in the two buffers. Like the reaction in H_2O, the net modest dimerization free energy of -8.5 kcal/mole in D_2O reflects large opposing enthalpies and entropies, albeit significantly more modest than those obtained in H_2O. These differences in the dimerization thermodynamics exist over the temperature range employed for the measurements (Figure 5). In both solvents the net unfavorable dimerization enthalpy reflects the penalty of desolvating the polar dimerization surface. However, this removal is energetically offset, in part, by formation of inter-solvent hydrogen bonds that accompanies its release to the bulk. The more modest net positive enthalpy measured in D_2O reflects the formation of enthalpically stronger bonds in the bulk than those formed by H_2O.[33] Likewise, the less favorable dimerization entropy in the heavier solvent may reflect the lower entropy of bulk D_2O relative to bulk H_2O, due to stronger hydrogen bonding of the former.[33] The very slow holoBirA dimerization kinetics estimated from analysis of sedimentation velocity data provides additional support for a significant role of solvent release in the process.[34] Simulations of protein aggregation indicate a high kinetic barrier to solvent release from polar side chains.[35] The favorable interaction of water with the charged and polar residues on the BirA dimerization surface should result in a similarly high barrier to dimer formation.

The solvent isotope effect on holoBirA dimerization thermodynamics is significantly larger than that measured for other protein association reactions. For example, measurements of the dimer-octamer equilibrium of β-lactoglobulin yielded enthalpies of -64 and -69 kcal/mol in H_2O and D_2O respectively[32]. Indeed, solvent isotope effects of the magnitude observed in this work have been reported only for protein folding [36], which may indicate a more significant role for solvent release in the holoBirA dimerization reaction than for other protein association reactions. Solvent isotope effects on protein folding and association reactions have previously been ascribed to stronger bonding resulting from exchange of deuterium for hydrogen in hydrogen bonding partners. [33; 37] Alternatively, the decreased flexibility observed for some proteins in D_2O may alter interaction thermodynamics [38; 39]. For BirA the absence of a solvent isotope effect on coupling between adenylate binding and dimerization points to solvent release as the major source of the distinct thermodynamic profiles measured in the two solvents.

Practical implications for Hydrogen Deuterium Exchange studies

Hydrogen-deuterium exchange measurements, detected by either mass spectrometry or NMR spectroscopy, are used to study protein folding, dynamics and interactions.[40; 41] The potential for solvent isotope perturbation of protein function has previously been suggested.[42; 43] Results reported in this work, which indicate that these effects can be large in magnitude, underscore the importance of performing appropriate controls to determine the functional effects of transferring a biomolecular system from H_2O to D_2O.

Acknowledgments

Financial Statement: This work was supported in part by NIH Grants R01GM46511 and S10RR15899 to DB.

References

1. Hodkinson PS, Elliott PA, Lad Y, McHugh BJ, MacKinnon AC, Haslett C, Sethi T. Mammalian NOTCH-1 activates beta1 integrins via the small GTPase R-Ras. J Biol Chem. 2007; 282:28991–29001. [PubMed: 17664272]
2. Layer JH, Miller SG, Weil PA. Direct transactivator-transcription factor IID (TFIID) contacts drive yeast ribosomal protein gene transcription. J Biol Chem. 2010; 285:15489–15499. [PubMed: 20189987]
3. Dickinson DJ, Robinson DN, Nelson WJ, Weis WI. alpha-catenin and IQGAP regulate myosin localization to control epithelial tube morphogenesis in Dictyostelium. Dev Cell. 2012; 23:533–546. [PubMed: 22902739]
4. Thirumalai D, Reddy G, Straub JE. Role of water in protein aggregation and amyloid polymorphism. Acc Chem Res. 2012; 45:83–92. [PubMed: 21761818]
5. Stranges PB, Kuhlman B. A comparison of successful and failed protein interface designs highlights the challenges of designing buried hydrogen bonds. Protein Sci. 2013; 22:74–82. [PubMed: 23139141]
6. Streaker ED, Beckett D. Coupling of protein assembly and DNA binding: biotin repressor dimerization precedes biotin operator binding. J Mol Biol. 2003; 325:937–948. [PubMed: 12527300]
7. Eisenstein E, Beckett D. Dimerization of the *Escherichia coli* biotin repressor:corepressor function in protein assembly. Biochemistry. 1999; 38:13077–13084. [PubMed: 10529178]
8. Streaker ED, Gupta A, Beckett D. The biotin repressor: thermodynamic coupling of corepressor binding, protein assembly, and sequence-specific DNA binding. Biochemistry. 2002; 41:14263–14271. [PubMed: 12450391]
9. Zhao H, Streaker E, Pan W, Beckett D. Protein-protein interactions dominate the assembly thermodynamics of a transcription repression complex. Biochemistry. 2007; 46:13667–13676. [PubMed: 17973495]
10. Khalil MT, Lauffer MA. Polymerization-depolymerization of tobacco mosaic virus protein. X. Effect of D20. Biochemistry. 1967; 6:2474–2480. [PubMed: 6058121]
11. Baldwin RL. Desolvation penalty for burying hydrogen-bonded peptide groups in protein folding. J Phys Chem B. 2010; 114:16223–16227. [PubMed: 20961078]
12. Wood Z, Weaver LH, Brown PH, Beckett D, Matthews BW. Co-repressor induced order and biotin repressor dimerization: a case for divergent followed by convergent evolution. J Mol Biol. 2006; 357:509–523. [PubMed: 16438984]
13. Saha RP, Bahadur RP, Pal A, Mandal S, Chakrabarti P. ProFace: a server for the analysis of the physicochemical features of protein-protein interfaces. BMC Struct Biol. 2006; 6:11. [PubMed: 16759379]
14. Krissinel E, Henrick K. Inference of macromolecular assemblies from crystalline state. J Mol Biol. 2007; 372:774–797. [PubMed: 17681537]
15. Courtenay ES, Capp MW, Anderson CF, Record MT Jr. Vapor pressure osmometry studies of osmolyte-protein interactions: implications for the action of osmoprotectants in vivo and for the interpretation of “osmotic stress” experiments in vitro. Biochemistry. 2000; 39:4455–4471. [PubMed: 10757995]
16. Kornblatt MJ, Kornblatt JA, Hui Bon Hoa G. The role of water in the dissociation of enolase, a dimeric enzyme. Arch Biochem Biophys. 1993; 306:495–500. [PubMed: 8215454]
17. Zhai Y, Okoro L, Cooper A, Winter R. Applications of pressure perturbation calorimetry in biophysical studies. Biophys Chem. 2011; 156:13–23. [PubMed: 21255903]
18. Chervenak MC, Toone EJ. A Direct Measure of the Contribution of Solvent Reorganization to the Enthalpy of Ligand-Binding. Journal of the American Chemical Society. 1994; 116:10533–10539.

19. Lane MD, Rominger KL, Young DL, Lynen F. The enzymatic synthesis of holotranscarboxylase from apotranscarboxylase and (+)-biotin. J Biol Chem. 1964; 239:2865–2871. [PubMed: 14216437]
20. Abbott J, Beckett D. Cooperative binding of the Escherichia coli repressor of biotin biosynthesis to the biotin operator sequence. Biochemistry. 1993; 32:9649–9656. [PubMed: 8373769]
21. Glasoe PK, Long FA. Use of Glass Electrodes to Measure Acidities in Deuterium Oxide. Journal of Physical Chemistry. 1960; 64:188–190.
22. Naganathan S, Beckett D. Nucleation of an allosteric response via ligand-induced loop folding. J Mol Biol. 2007; 373:96–111. [PubMed: 17765263]
23. Adikaram PR, Beckett D. Functional versatility of a single protein surface in two protein:protein interactions. J Mol Biol. 2012; 419:223–233. [PubMed: 22446587]
24. Gill SC, von Hippel PH. Calculation of protein extinction coefficients from amino acid sequence data. Analytical Biochemistry. 1989; 182:319–326. [PubMed: 2610349]
25. Johnson ML, Correia JJ, Yphantis DA, Halvorson HR. Analysis of data from the analytical ultracentrifuge by nonlinear least-squares techniques. Biophys J. 1981; 36:575–588. [PubMed: 7326325]
26. Martin WG, Winkler CA, Cook WH. Partial Specific Volume Measurements by Differential Sedimentation. Can J Chem. 1959; 37:1662–1670.
27. Edelstein SJ, Schachman HK. The simultaneous determination of partial specific volumes and molecular weights with microgram quantities. J Biol Chem. 1967; 242:306–311. [PubMed: 6016615]
28. Lee JJ, Berns DS. Protein aggregation. The effect of deuterium oxide on large protein aggregates of C-phycocyanin. Biochem J. 1968; 110:465–470. [PubMed: 5701676]
29. Woodfin BM, Henderson RF, Henderson TR. Effects of D2O on the association-dissociation equilibrium in subunit proteins. J Biol Chem. 1970; 245:3733–3737. [PubMed: 5531188]
30. Aune KC, Goldsmith LC, Timasheff SN. Dimerization of alpha-chymotrypsin. II. Ionic strength and temperature dependence. Biochemistry. 1971; 10:1617–1622. [PubMed: 4325604]
31. Paglini S, Lauffer MA. Polymerization-depolymerization of tobacco mosaic virus protein. XI. Osmotic pressure studies of solutions in water and in deuterium. Biochemistry. 1968; 7:1827–1835. [PubMed: 5650382]
32. Baghurst PA, Nichol LW, Sawyer WH. The effect of D 2 O on the association of -lactoglobulin A. J Biol Chem. 1972; 247:3199–3204. [PubMed: 5063681]
33. Nemethy G, Scheraga HA. Structure of Water + Hydrophobic Bonding in Proteins .4. Thermodynamic Properties of Liquid Deuterium Oxide. Journal of Chemical Physics. 1964; 41:680. &.
34. Zhao H, Beckett D. Kinetic partitioning between alternative protein-protein interactions controls a transcriptional switch. J Mol Biol. 2008; 380:223–236. [PubMed: 18508076]
35. Reddy G, Straub JE, Thirumalai D. Dry amyloid fibril assembly in a yeast prion peptide is mediated by long-lived structures containing water wires. Proc Natl Acad Sci U S A. 2010; 107:21459–21464. [PubMed: 21098298]
36. Makhatadze GI, Clore GM, Gronenborn AM. Solvent isotope effect and protein stability. Nat Struct Biol. 1995; 2:852–855. [PubMed: 7552708]
37. Cho Y, Sagle LB, Iimura S, Zhang Y, Kherb J, Chilkoti A, Scholtz JM, Cremer PS. Hydrogen bonding of beta-turn structure is stabilized in D(2)O. J Am Chem Soc. 2009; 131:15188–15193. [PubMed: 19919159]
38. Cioni P, Strambini GB. Effect of heavy water on protein flexibility. Biophys J. 2002; 82:3246–3253. [PubMed: 12023248]
39. Tehei M, Madern D, Pfister C, Zaccai G. Fast dynamics of halophilic malate dehydrogenase and BSA measured by neutron scattering under various solvent conditions influencing protein stability. Proc Natl Acad Sci U S A. 2001; 98:14356–14361. [PubMed: 11734642]
40. Konermann L, Pan J, Liu YH. Hydrogen exchange mass spectrometry for studying protein structure and dynamics. Chem Soc Rev. 2011; 40:1224–1234. [PubMed: 21173980]

41. Lee YH, Goto Y. Kinetic intermediates of amyloid fibrillation studied by hydrogen exchange methods with nuclear magnetic resonance. Biochim Biophys Acta. 2012; 1824:1307–1323. [PubMed: 22885025]

42. Sackett DL, Chernomordik V, Krueger S, Nossal R. Use of small-angle neutron scattering to study tubulin polymers. Biomacromolecules. 2003; 4:461–467. [PubMed: 12625746]

43. Prasannan CB, Artigues A, Fenton AW. Monitoring allostery in D2O: a necessary control in studies using hydrogen/deuterium exchange to characterize allosteric regulation. Anal Bioanal Chem. 2011; 401:1083–1086. [PubMed: 21701851]

44. DeLano, WL. The PyMOL Molecular Graphics System, Version 1.2r3pre. Schrödinger, LLC; 2002.

Abbreviations

BirA	*E. coli* bifunctional biotin repressor/biotin protein ligase
holoBirA	BirA bound to bio-5'-AMP
apoBirA	ligand-free BirA
bio-5'-AMP	biotinoyl-5'-adenosine monophosphate
Tris	tris (hydroxymethyl) amino methane
SDS	sodium dodecyl sulfate
SB	Standard Buffer: 10 mM Tris, 200 mM KCl, 2.5 mM $MgCl_2$, pH 7.5 at the working temperature
SB:H_2O	Standard Buffer prepared in H_2O
SB:D_2O	Standard Buffer prepared in D_2O

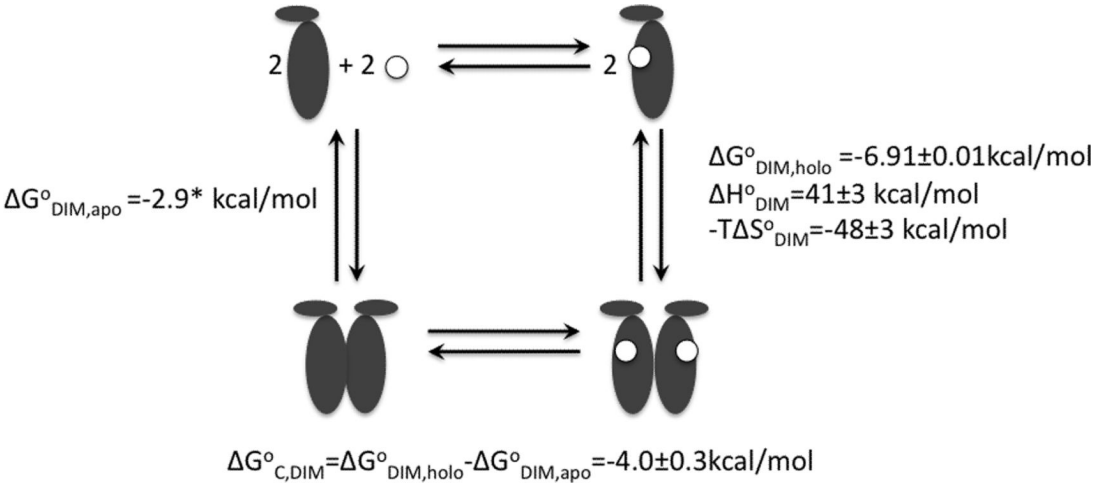

Figure 1.

Thermodynamic cycle illustrating the linkage between BirA dimerization and bio-5'-AMP binding. The coupling, $\Delta G^{\circ}_{C,DIM}$, is calculated from the difference in the measured dimerization free energy of bio-5'-AMP-bound or holoBirA, and unliganded or apoBirA, $\Delta G^{\circ}_{DIM,holo}-\Delta G^{\circ}_{DIM,apo}$. The thermodynamic parameters for holoBirA dimerization are shown on the right of the cycle. White circle: bio-5'-AMP, Grey image: BirA. *The free energy of apoBirA dimerization in 200 mM KCl is calculated from the value measured in 50 mM KCl and the measured effect of salt concentration on holoBirA dimerization.[8; 9]

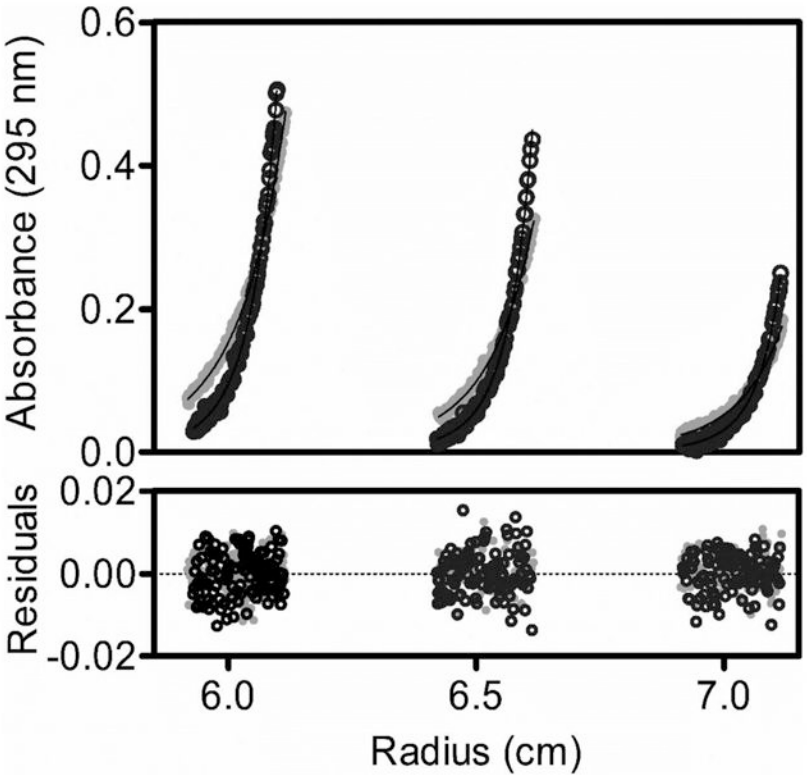

Figure 2.

Sedimentation equilibrium measurements of wild type holoBirA in SB:D_2O at 20°C. HoloBirA prepared at 23, 15 and 7.5 μM, from left to right, were centrifuged at 18,000 ( ) and 24,000 ( )rpm. The lines correspond to the best-fit of nine data sets to a monomer-dimer model. For clarity, only six data sets are shown with the residuals of the fit.

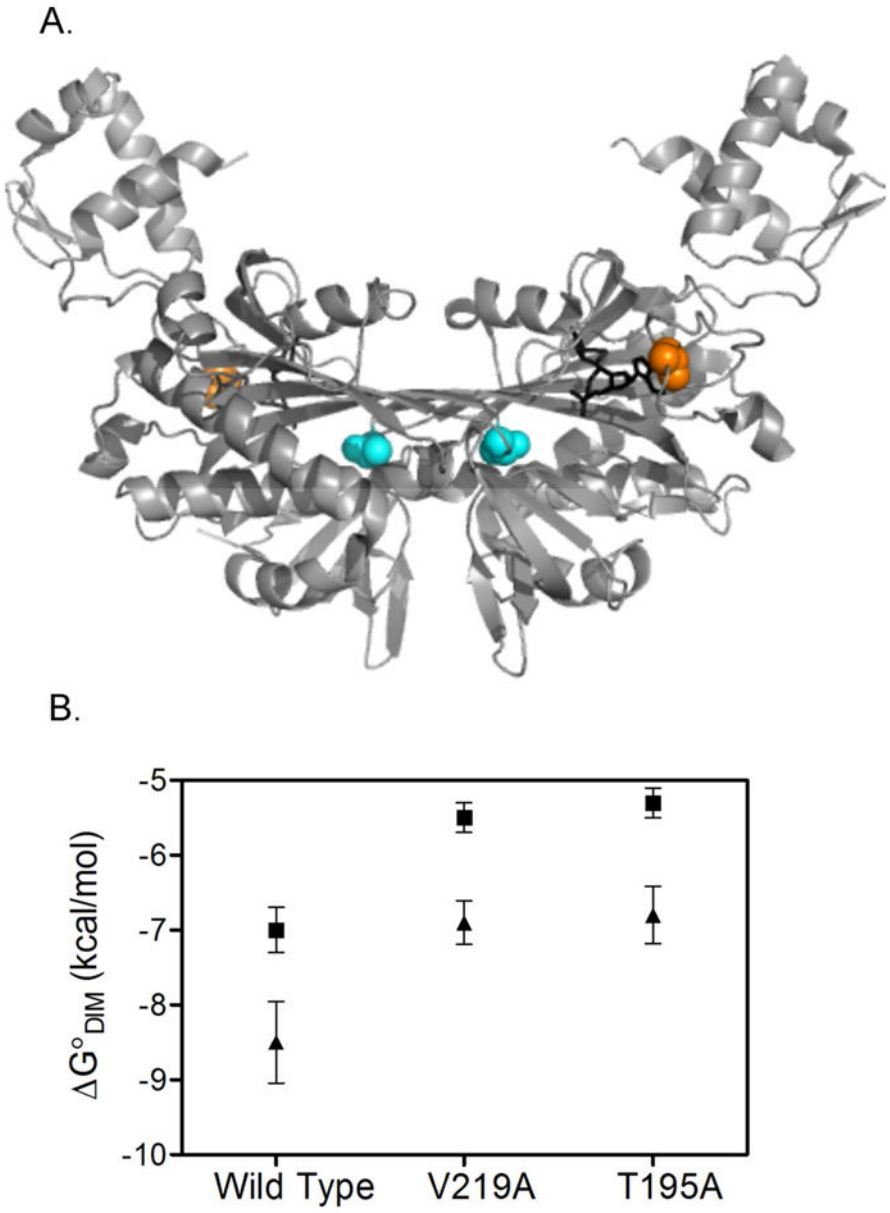

Figure 3.

A. Locations of alanine substitutions in the BirA structure. The T195A (cyan) substitution is at the dimerization interface and the V219A (orange) is in a loop that folds over the adenosine moiety and is on the outside surface of the dimer. The model was constructed in PyMol using the input file 2EWN.[12; 44] B. Energetic effects of transfer of the dimerization reaction from SB:H_2O to SB:D_2O: The Gibbs free energies of dimerization in H_2O (■) and D_2O (⑩) indicate a consistent enhancement of -1.5 kcal/mole.

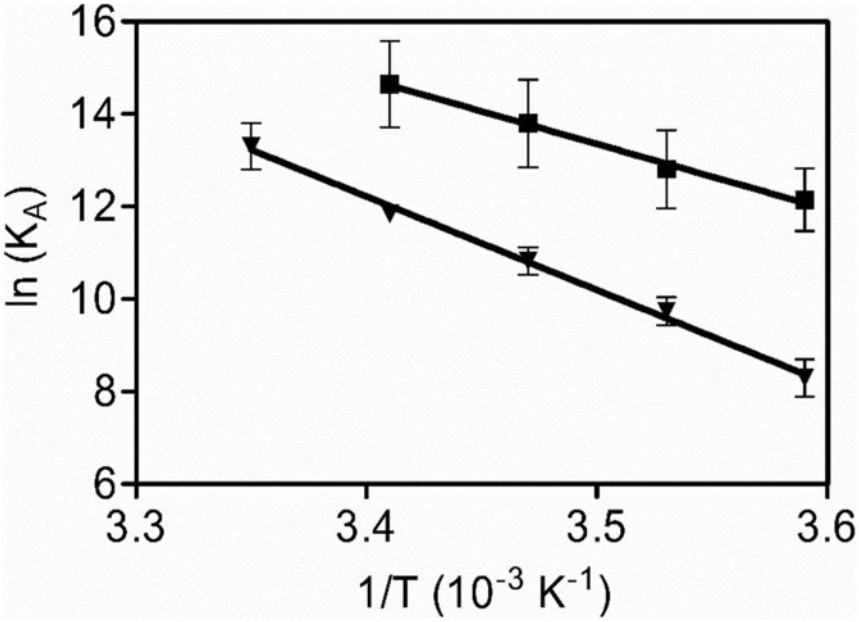

Figure 4.
Van't Hoff analysis of the temperature-dependence of the equilibrium constant for holoBirA dimerization in SB:D_2O(■) and SB:H_2O (▼). The lines correspond to the best fits of the data to the van't Hoff equation. The data obtained in SB:H_2O were previously described.[9]

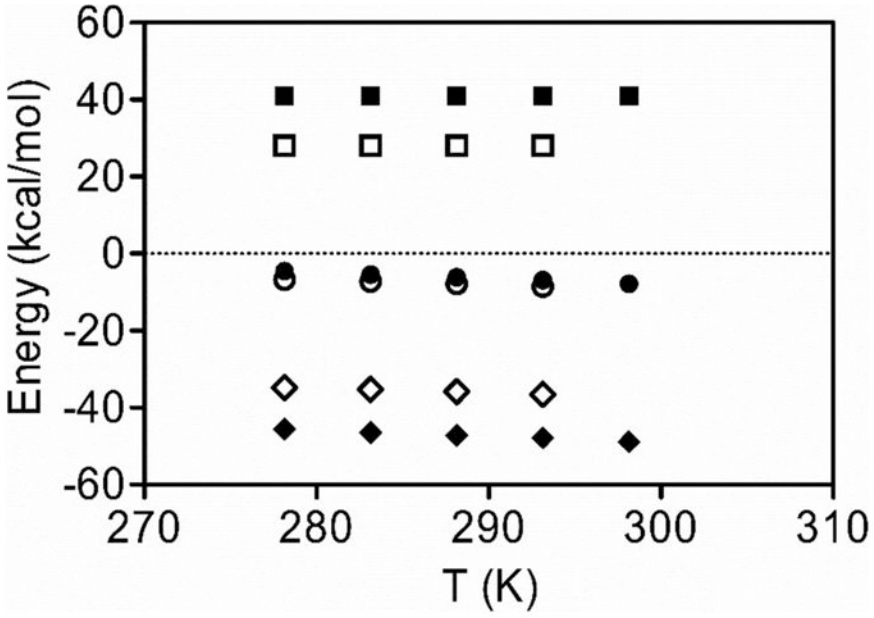

Figure 5.

Thermodynamic signatures for holoBirA dimerization in SB:H_2O and SB:D_2O. The energetic terms in H_2O and D_2O are $\Delta G°_{DIM}$ (●,◯), $\Delta H°_{dim}$(■, □) and $-T\Delta S°_{DIM}$ (◆,◊). The values in SB:H_2O were previously published.[9] On the scale used for the graph the estimated errors in the values are within the symbols.

Table 1

Solvent isotope effects on BirA dimerization

Solvent		H_2O		D_2O	
BirA Variant	K_{Dim} (M)[a],	$\Delta G°_{Dim}$ (kcal/mol)[b]	K_{Dim} (M)[a]	$\Delta G°_{Dim}$ (kcal/mol)[b]	$\Delta\Delta G°_{Dim}$ (kcal/mol)[b,c]
Apo wild-type		(−2.8)[d]	$6 \pm 1 \times 10^{-4}$	−4.3± 0.1	(−1.5)[d]
Holo wild-type	$6 \pm 2 \times 10^{-6}$	−7.0 ± 0.3	$5 \pm 5 \times 10^{-7}$	−8.5± 0.5	−1.5 ± 0.6
V219A	$8 \pm 1 \times 10^{-5}$	−5.5 ± 0.2	$7 \pm 4 \times 10^{-6}$	−6.9± 0.3	−1.4 ± 0.4
T195A[e]	$10 \pm 4 \times 10^{-5}$	−5.3 ± 0.2	$9 \pm 7 \times 10^{-6}$	−6.8± 0.4	−1.5 ± 0.4

[a] Standard errors reported are from two independent experiments.

[b] Standard error propagation methods were used to determine the uncertainties for each reported value.

[c] $\Delta\Delta G°_{DIM} = \Delta G°_{DIM(SB:D_2O)} - \Delta G°_{DIM(SB:H_2O)}$

[d] The values provided for apoBirA were calculated using the equilibrium dissociation constant measured in SB:H_2O containing 50 mM KCl and assuming identical dependencies of apo- and holoBirA dimerization on KCl concentration.[8; 9]

[e] The equilibrium constant and Gibbs free energy of dimerization in H_2O for the T195A variant were previously reported.[23]